





Article

Synthesis, Characterization and DFT Calculations of 4,5,12- and 1,8,12-trichloro-9,10-dihydro-9,10-ethanoanthracene-12-carbonitriles

Mujeeb A. Sultan ^{1,*} , Usama Karama ¹, Abdulrahman I. Almansour ¹, Saied M. Soliman ^{2,3} , Hazem A. Ghabbour ^{4,5}  and Yahia N. Mabkhot ^{1,*} 

¹ Chemistry Department, College of Science, King Saud University, P.O. Box 2455, Riyadh 11451, Saudi Arabia; Karama@ksu.edu.sa (U.K.); almansor@ksu.edu.sa (A.I.A.)

² Department of Chemistry, Rabigh College of Science and Art, P.O. Box 344, Rabigh 21911, Saudi Arabia; saied1soliman@yahoo.com

³ Department of Chemistry, Faculty of Science, Alexandria University, P.O. Box 426, Ibrahimia, 21321 Alexandria, Egypt

⁴ Department of Pharmaceutical Chemistry, College of Pharmacy, King Saud University, P.O. Box 2457, Riyadh 11451, Saudi Arabia; ghabbourh@yahoo.com

⁵ Department of Medicinal Chemistry, Faculty of Pharmacy, University of Mansoura, Mansoura 35516, Egypt

* Correspondence: alhosami1983@yahoo.co.uk (M.A.S.); yahia@ksu.edu.sa (Y.N.M.); Tel.: +966-59-633-6123 (M.A.S.); +966-11-467-5898 (Y.N.M.)

Academic Editor: Jacob Overgaard

Received: 6 July 2017; Accepted: 15 August 2017; Published: 25 August 2017

Abstract: The chlorinated ethanoanthracenes: 4,5,12- and 1,8,12-(trichloro-9,10-dihydro-9,10-ethanoanthracene-12-carbonitriles) (**1** and **2**), which are regioisomers, were synthesized and characterized using nuclear magnetic resonance (¹H- and ¹³C-NMR) and infrared (IR) spectroscopic techniques. The structure of isomer **1** was further confirmed using a single-crystal X-ray technique. The relative stabilities of the title compounds were calculated using the density functional theory (DFT) method on the basis of their total energies and thermodynamic parameters. Isomer **1** is thermodynamically more stable than isomer **2** in the gas phase and in solution. The calculated molecular geometry of isomer **1** agreed well with the experimental X-ray structure. The atomic charge distribution at the different atomic sites was calculated using natural bond orbital analysis. Isomer **2** was predicted to be more polar than isomer **1**.

Keywords: synthesis; ethanoanthracene; Diels-Alder cycloaddition; X-ray; DFT

1. Introduction

Anthracenes are important compounds for the dye production, the development of organic electronics, and as intermediates for chemotherapeutic agents [1–4]. Halogenated anthracenes are useful in the treatment of allergies, inflammations and tumors [5–8]. Ethanoanthracene derivatives represent an important class of bioactive molecules that show a wide range of pharmaceutical activities including antidepressants [9], anti-proliferative agent against Burkitt's lymphoma cell lines [10], and show activity against multi-drug resistance (MDR) in cancer cells and the malaria strain *Plasmodium falciparum* [11–13]. The Diels-Alder cycloaddition is one of the most atomically economic and valuable synthetic reaction, which has efficiently employed in the synthesis of tetracyclic, in particular bicyclo [2.2.2], compounds [14]. It is a [4 + 2] π cycloaddition where a 4π conjugated diene reacts with a 2π alkene dienophile to form six-member system where two σ -bonds and a new π -bond are forming at the expense of three π -bonds, with good control over regio- and stereochemical properties. The German Chemists Diels and Alder were awarded the Nobel Prize in

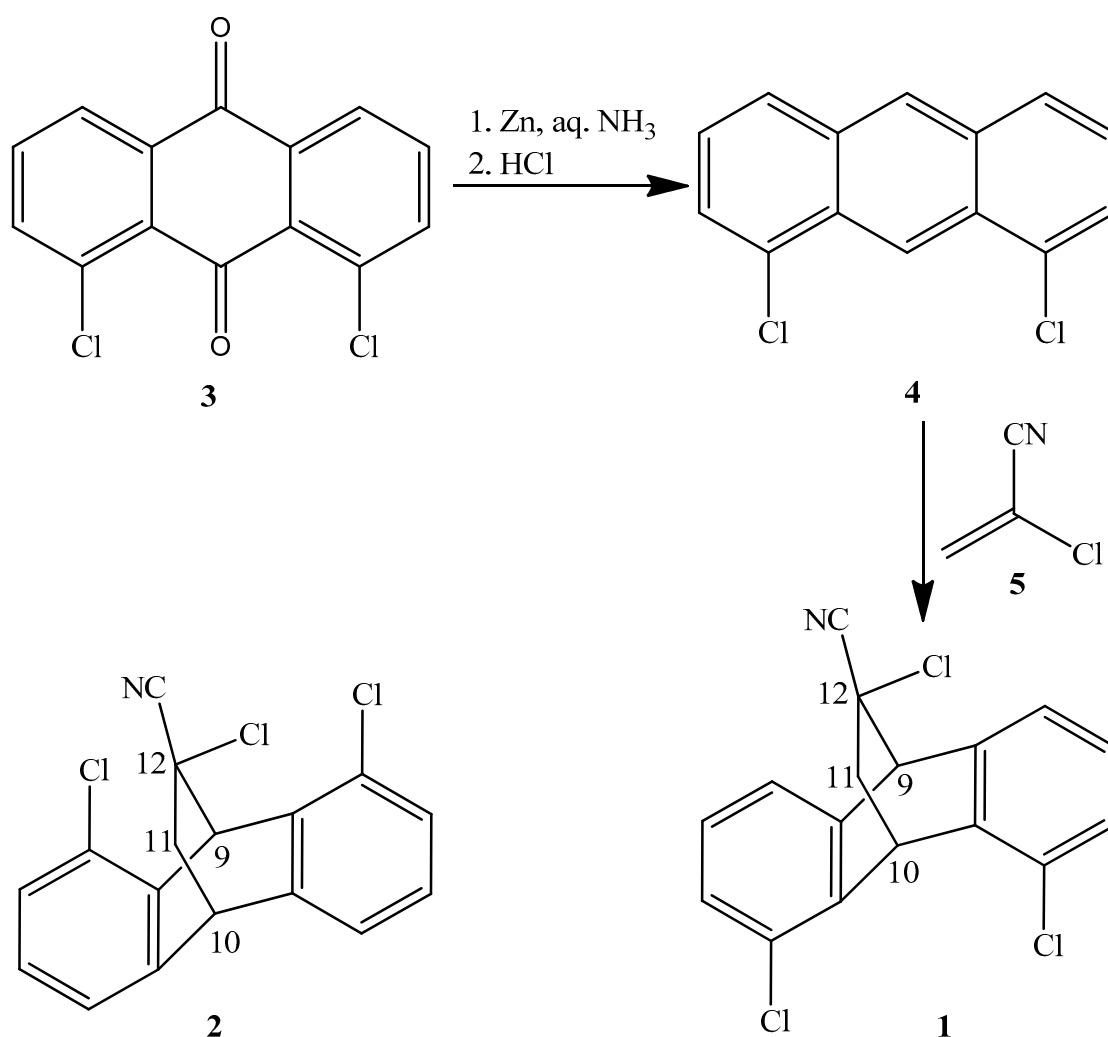
chemistry for this reaction in 1950 [15–17]. The functionalization of anthracene has been described extensively. It is well known that anthracene is a good diene in Diels-Alder reactions, since its central ring is electron rich, with largest coefficients at C9 and C10 [18–27]. Based on the above, we expected that the presence of chlorine atoms in ethanoanthracene molecules would be of interest in the context of anticancer drug discovery. In continuation of our interest in [4 + 2] Diels-Alder cycloaddition, we report in this article the preparation of novel chlorinated ethanoanthracenes, 4,5,12- and 1,8,12-trichloro-9,10-dihydro-9,10-ethanoanthracene-12-carbonitriles (**1** and **2**) as regioisomers of the reaction between 1,8-dichloroanthracene **4** and 2-chloroacrylonitrile **5** under xylene reflux condition. The structures of these isomers were elucidated using nuclear magnetic resonance (¹H- and ¹³C-NMR) and infrared (IR) spectroscopic techniques. Furthermore the structure of isomer **1** was further confirmed using a single crystal X-ray technique. Density functional theory (DFT) calculations at the B3LYP level of theory and with the 6-31G(d,p) basis set were used to deduce the relative stabilities, molecular structures and electronic properties of **1** and **2**.

2. Results and Discussion

2.1. Synthesis

The synthetic route towards **1** and **2** is shown in Scheme 1. As showing in Scheme 1, **1** and **2** can be prepared as a mixture in a 2:1 ratio through the the reduction of the carbonyl groups of 1,8-dihaloanthraquinone **3** with zinc powder in 28% aqueous ammonia, treatment with 12 M HCl to afford 1,8-dichloroanthracene **4**, and then a Diels-Alder cycloaddition reaction between **4** and 2-chloroacrylonitrile **5** in xylene under reflux conditions.

In the Diels-Alder cycloaddition reaction between **4** and **5**, the formation of isomer **1** is favored and this may be because isomer **1** is more stable than isomer **2**, as corroborated by theoretical calculations and indicated by experimental results of similar reactions [28,29]. The structures of these regioisomers were elucidated using ¹H- and ¹³C-NMR, and IR spectroscopic techniques. Regioisomers **1** and **2** could be clearly distinguished after the ¹H-NMR peaks were assigned. The bridge-head protons, H-9 and H-10, of isomer **1** appearing at δ 4.68 ppm as a singlet and at δ 5.35 ppm as a triplet, the latter presenting a coupling constant (*J*) of 2.2 Hz. Whereas the bridge-head protons H-9 and H-10 of the isomer **2** appearing at δ 5.83 ppm as a singlet and at δ 4.36 ppm as a triplet, the latter also presenting a coupling constant (*J*) of 2.2 Hz. The downfield shifting of H-10, relative to H-9, for isomer **1** is the result of the deshielding effect of the chlorine atoms, since they are in positions **4** and **5** and are very close to H-10. The clear downfield shifting of H-9, relative to H-10, in isomer **2** is the result of the deshielding effects of the chlorine atoms and nitrile group, since the chlorine atoms are in positions **4**, **5**, and **12** and the CN group in position **12** and are very close to H-9. Furthermore, the three-dimensional structure of isomer **1** was confirmed using a single-crystal X-ray technique.



Scheme 1. Synthesis of regioisomers **1** and **2**.

2.2. X-ray Single Crystal Structure Analysis of Isomer **1**

Isomer **1** was crystallized from dichloromethane as single colorless plate crystals using the slow evaporation technique and analyzed using X-ray diffraction. An Oak Ridge Thermal Ellipsoid Plot (ORTEP) drawing of the molecular structure of isomer **1** at a 40% probability, with its numbering scheme, is shown in Figure 1. X-ray diffraction data and refinements are presented in Table 1. Isomer **1** crystallized in the monoclinic space group $P2_1/n$ and was found to adopt a V shape with the two phenyl ring planes making a dihedral angle of 125.26° . The molecules were packed in the crystal structure via two weak intermolecular H...Cl interactions, C13—H13A...Cl1 and C13—H13A...Cl2. The H...A distances were 2.75 and 2.77 Å, respectively in Figure 2.

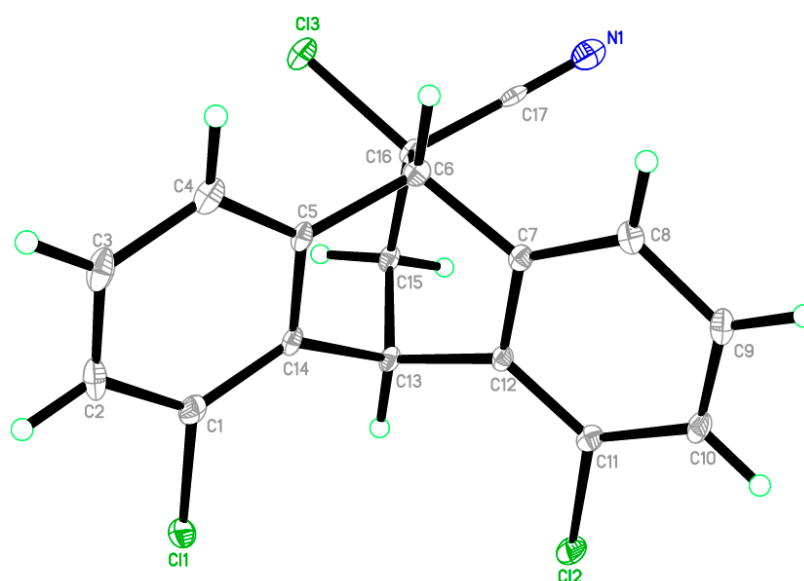


Figure 1. ORTEP drawing of isomer **1** and its numbering scheme. Thermal ellipsoids are drawn at the 40% probability level at 100 K.

Table 1. Crystal structure and refinement data for isomer **1**.

Crystal Data	
Chemical formula	C ₁₇ H ₁₀ Cl ₃ N
Formula weight	334.61
Crystal system, space group	Monoclinic, <i>P</i> 2 ₁ / <i>n</i>
Temperature (K)	100
<i>a</i> , <i>b</i> , <i>c</i> (Å)	9.2332 (5), 12.4617 (6), 12.8375 (7)
β (°)	105.678 (2)
<i>V</i> (Å ³)	1422.15 (13)
<i>Z</i>	4
Radiation type	Mo <i>K</i> α
μ (mm ^{−1})	0.63
Crystal size (mm)	0.55 × 0.38 × 0.12
Data collection	
Diffractometer	Bruker APEX-II D8 VENTURE diffractometer
Absorption correction	Multi-scan, SADABS Bruker 2014
T _{min} , T _{max}	0.723, 0.926
No. of measured, independent and observed [<i>I</i> > 2σ(<i>I</i>)] reflections	16403, 3250, 2462
R _{int}	0.089
Refinement	
R[<i>F</i> ² > 2σ(<i>F</i> ²)], wR(<i>F</i> ²), <i>S</i>	0.049, 0.124, 1.04
No. of reflections	3250
No. of parameters	190
No. of restraints	0
H-atom treatment	H atoms treated by a mixture of independent and constrained refinements
Δρ _{max} , Δρ _{min} (e Å ^{−3})	0.49, −0.61

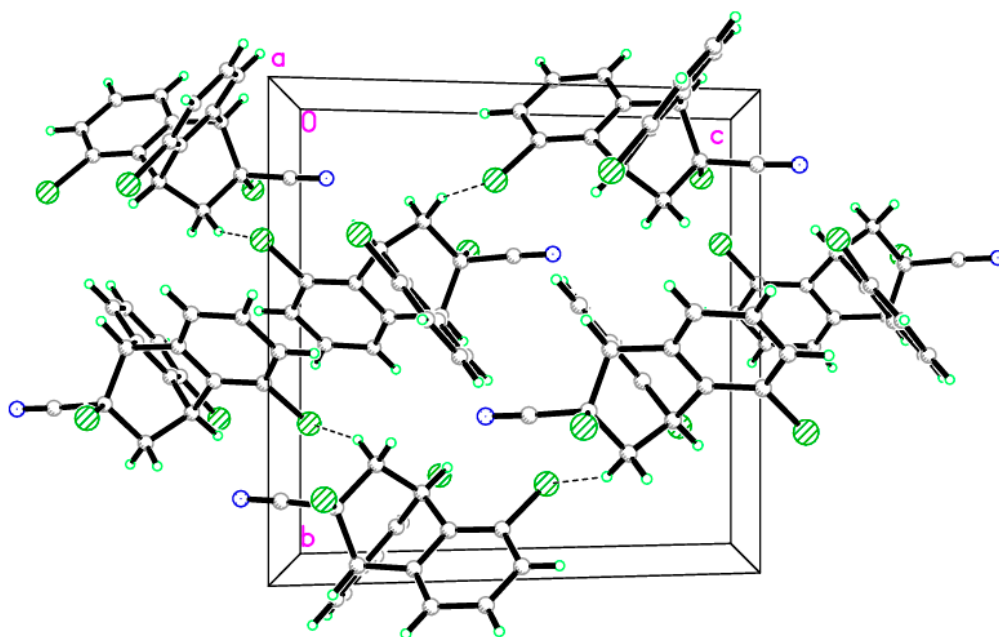


Figure 2. Molecular packing of isomer 1 with hydrogen bonds shown; the hydrogen bonds are drawn as dashed lines along the *c* axis.

2.3. Theoretical Calculations

2.3.1. Energetic and Optimized Geometry

The total energies and thermodynamic parameters of the studied regioisomers, **1** and **2**, are listed in Table 2. It is clear that isomer **1** is more stable than isomer **2** by only 1.16 and 0.84 Kcal/mol in gas phase and in solution (chloroform as solvent), respectively. The small energy difference between **1** and **2** sheds light on their formation as reaction products. Moreover, the difference in Gibbs free energy ($G_1 - G_2$) is negative, which indicates that isomer **1** is thermodynamically more stable than isomer **2** both in the gas phase and in solution.

Table 2. Energies and thermodynamic parameters of the studied isomers.

	Gas		CHCl ₃	
	Isomer 1	Isomer 2	Isomer 1	Isomer 2
E (a.u.)	−2089.1773	−2089.1753	−2089.1885	−2089.1871
ZPVE (a.u.)	0.222732	0.222619	0.221657	0.221574
Ecorr (a.u.)	−2088.95453	−2088.95268	−2088.96683	−2088.96549
ΔE (kcal/mol)	−1.16290		−0.84192	
H (a.u.)	−2088.9369	−2088.935	−2088.9492	−2088.9478
S (cal/mol K)	131.624	131.532	131.826	131.812
G (a.u.)	−2088.9994	−2088.9975	−2089.0118	−2089.0104
ΔG (kcal/mol)	−1.194778		−0.8571779	

The optimized bond lengths and angles obtained for isomer **1** using the B3LYP method with the 6-31G(d,p) basis set are given in Table 3 while the optimized structure is given in Figure 3. Both isomers have a C_1 point group. The calculated geometric parameters (bond distances and bond angles) of isomer **1** showed good agreement with the structural parameters obtained from the crystallographic information file (CIF). The correlations between the calculated and experimental bond distances and angles were good, with correlation coefficients (R^2) of 0.9957 and 0.9974, respectively. Moreover, the calculated root mean square deviations (RMSDs) of the bond distances and bond angles were

0.046 Å and 4.3°, respectively. As shown in Figure 3, the overlay of the calculated and experimental structure is nearly perfect and the deviations from each other are very small.

Table 3. Calculated and experimental bond distances (Å) and angles (°) of isomer 1.

Parameter	Calc.	X-ray	Parameter	Calc.	X-ray
R(1-5)	1.761	1.746	A(6-5-26)	120.7	120.8
R(2-22)	1.760	1.743	A(5-6-8)	119.7	119.4
R(3-30)	1.841	1.811	A(5-26-12)	118.7	118.4
R(5-6)	1.398	1.395	A(5-26-24)	128.1	127.8
R(5-26)	1.392	1.383	A(6-8-10)	120.6	120.8
R(6-8)	1.394	1.389	A(8-10-12)	119.0	118.6
R(8-10)	1.398	1.388	A(10-12-13)	125.8	125.4
R(10-12)	1.390	1.383	A(10-12-26)	121.3	121.9
R(12-13)	1.517	1.517	A(13-12-26)	112.9	112.7
R(12-26)	1.405	1.396	A(12-13-15)	108.2	108.6
R(13-15)	1.521	1.519	A(12-13-30)	107.4	106.6
R(13-30)	1.578	1.566	A(12-26-24)	113.2	113.8
R(15-16)	1.390	1.382	A(15-13-30)	105.6	104.6
R(15-23)	1.406	1.398	A(13-15-16)	125.8	125.5
R(16-18)	1.398	1.394	A(13-15-23)	112.9	113.1
R(20-22)	1.398	1.398	A(13-30-27)	108.9	110.1
R(22-23)	1.392	1.386	A(13-30-31)	110.3	109.2
R(23-24)	1.520	1.514	A(16-15-23)	121.4	121.4
R(24-26)	1.519	1.519	A(15-16-18)	119.0	118.9
R(24-27)	1.561	1.550	A(15-23-22)	118.7	118.7
R(27-30)	1.566	1.553	A(15-23-24)	113.2	113.4
R(30-31)	1.465	1.511	A(16-18-20)	120.6	120.9
A(1-5-6)	118.7	118.8	A(18-20-22)	119.7	119.3
A(1-5-26)	120.6	120.4	A(20-22-23)	120.7	120.8
A(2-22-20)	118.7	118.5	A(22-23-24)	128.2	127.9
A(2-22-23)	120.6	120.8	A(23-24-26)	107.4	107.7
A(3-30-13)	109.3	105.0	A(23-24-27)	106.9	106.9
A(3-30-27)	110.7	110.2	A(26-24-27)	106.9	106.1
A(3-30-31)	105.9	105.0	A(24-27-30)	109.4	108.9
A(4-31-30)	179.2	177.4	A(27-30-31)	111.8	112.5

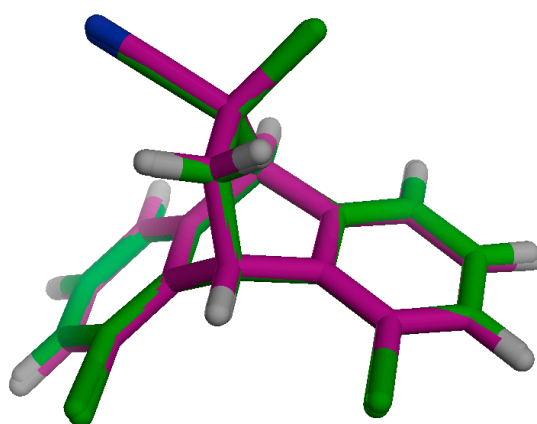


Figure 3. Overlay of the optimized and experimental molecular structure of isomer 1.

2.3.2. HOMO and LUMO Analysis

The highest occupied molecular orbital (HOMO) and lowest unoccupied molecular orbital (LUMO) are important electronic parameters. Their relative energies are related to the ability of

molecule to gain or lose electrons. The $\Delta E = E_{\text{LUMO}} - E_{\text{HOMO}}$ value represents the minimum amount of energy required for the electronic transition. The energies and shapes of their electron densities are also useful for predicting the positions and assigning the electronic transition bands observed in the electronic absorption spectra. Figure 4 shows the shapes of the frontier molecular orbitals calculated for the optimized structure at the same level of theory. The HOMO and LUMO levels are mainly distributed over the π -system of the molecule for both isomers. From this point of view, the electron transfer is considered a π - π^* transition. The calculated E_{HOMO} and E_{LUMO} values are given in Figure 4. Both the HOMO and LUMO levels are lower in energy for isomer 1 than for isomer 2. Moreover the energy gap in the former is higher. The transition energies from the HOMO to the LUMO are 5.6274 and 5.6260 eV for 1 and 2, respectively.

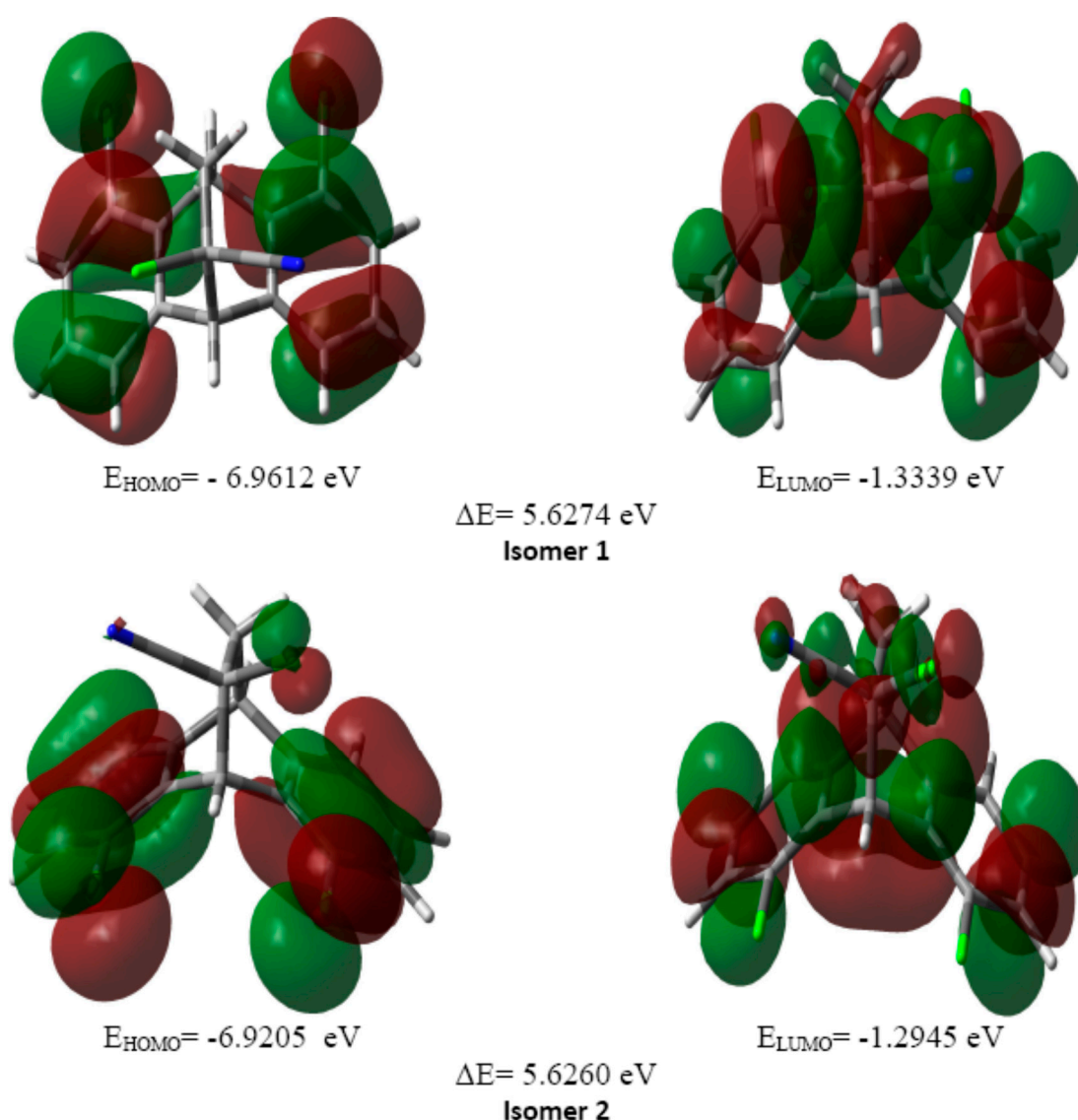


Figure 4. Molecular orbital surfaces of the HOMO and LUMO energy levels of regioisomers 1 and 2 computed at the B3LYP/6-31G(d,p) level.

2.3.3. Atomic Charges

The atomic charge distribution at the different atomic sites of the studied isomers are shown in Figure 5. Regioisomers 1 and 2 have nearly identical natural atomic charge values. It is clear that all carbon atoms have negative natural charge values for both isomers. In contrast, the H atoms

are electropositive, and the aliphatic protons have more positive charge than any of the aromatic ones. The most negative atom is the nitrogen of the nitrile group, while the most positively-charged atoms are those related to the aliphatic H atoms. A molecular electrostatic potential (MEP) diagram is useful for predicting the most positive (electrophilic) and negative (nucleophilic) regions in a molecule. The positive (blue) and negative (red) regions are the most reactive sites for nucleophilic and electrophilic attack, respectively. As shown in Figure 6, there is no doubt that the phenyl rings in both isomers are highly electrophilic. Moreover, the MEP values revealed that the most negative region is around the nitrogen atom of the nitrile group, which acts as a nucleophilic center, while the most positive region is around the aliphatic protons (electrophile). The dipole moment is a relevant electronic property that depends on the charge distribution. Interestingly, isomer 2 (6.31 D) was found to be more polar than isomer 1 (3.45 D). The presence of the electronegative atoms (Cl and N) on the same side leads to a more polar structure.

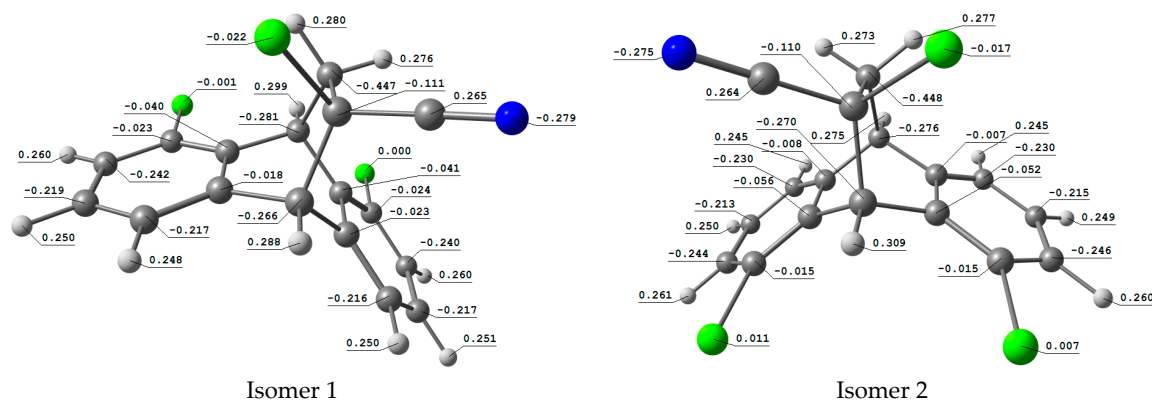


Figure 5. Atomic charge distributions at different atomic sites of regioisomers 1 and 2.

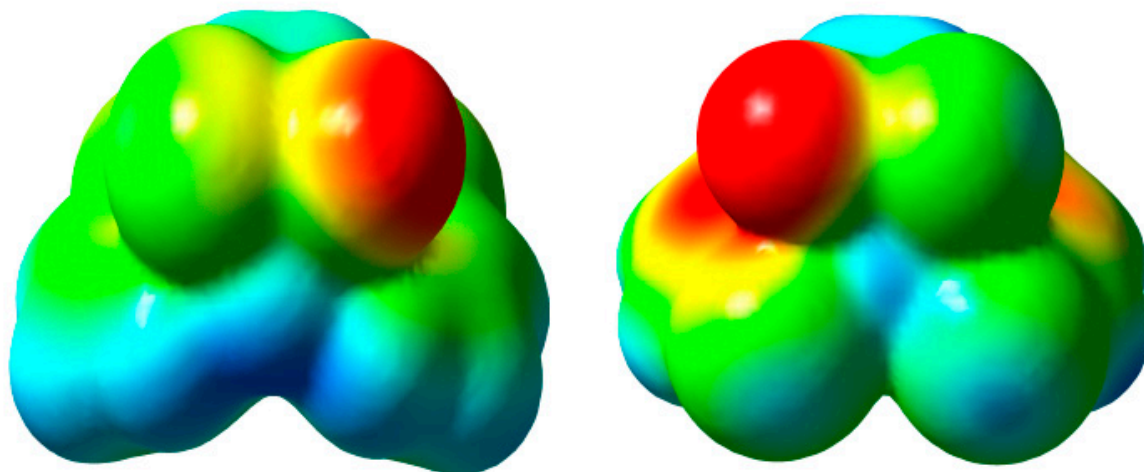


Figure 6. Electron density maps based on the molecular electrostatic potential of regioisomers 1 and 2.

3. Materials and Methods

3.1. Synthesis

3.1.1. General Notes

All chemicals were purchased from Sigma-Aldrich and used without further purification. Melting points ($^{\circ}\text{C}$) were determined using a KSP1N Melting Point Meter (Krüss, Germany) and are uncorrected.

IR spectra were recorded with KBr discs using FT-IR Bruker Vertex 70 Spectrometer (Bruker, Germany) and the data are expressed in wave numbers (ν cm^{-1}). ^1H and ^{13}C nuclear magnetic resonance (NMR) spectra were recorded on a JEOL 400 MHz NMR spectrometer (JEOL, Tokyo, Japan) in CDCl_3 , and chemical shifts are expressed in δ (ppm) and coupling constants (J) are given in Hz.

3.1.2. Synthesis of 1,8-dichloroanthracene **4**

The intermediate 1,8-dichloroanthracene, **4**, was synthesized from the commercially available starting material 1,8-dichloroanthraquinone **3** according to procedure from the literature [26,30].

3.1.3. Synthesis of 4,5,12-trichloro-9,10-dihydro-9,10-ethanoanthracene-12-carbonitrile **1** and 1,8,12-Trichloro-9,10-dihydro-9,10-ethanoanthracene-12-carbonitrile **2**

2-Chloroacrylonitrile **5** (200 μL , 2.5 mmol) was added to a solution of **4** (200 mg, 0.81 mmol) in xylene (1 mL). The mixture was stirred and refluxed at 95 $^\circ\text{C}$ for 48h and then cooled to room temperature, then the solvent was removed in vacuo. The residue was purified via preparative paper chromatography using ethyl acetate/hexane (1:5) to afford regioisomers **1** (130 mg, 48%) and **2** (65 mg, 24%) with the following characterization data:

Isomer 1: white powder; mp 170 $^\circ\text{C}$; IR (KBr): $\nu = 3444, 2989, 2945, 2853, 2441, 1578, 1456, 1436, 1188, 1166, 1069, 1047, 976, 947, 830, 786, 737, 701, 671, 647, 590, 477$ cm^{-1} ; $^1\text{H-NMR}$ (CDCl_3 , 400 MHz): $\delta = 2.27$ (dd; $J = 2.2, 13.92$ Hz, 1H, H-12), 2.74 (dd; $J = 2.2, 13.92$ Hz, 1H, H-12), 4.68 (s; 1H, H-9), 5.35 (t; $J = 2.2$ Hz, 1H, H-10), 7.08–7.30 (m; 6H, ArH) ppm; $^{13}\text{C-NMR}$ (CDCl_3 , 100 MHz): $\delta = 36.4, 45.0, 45.1, 54.7, 119.0, 124.5, 124.6, 125.4, 125.5, 128.4, 128.8, 129.8, 130.0, 137.7, 138.5, 138.7, 139.3$ ppm.

Isomer 2: white powder; mp 150 $^\circ\text{C}$; IR (KBr): $\nu = 3439, 2967, 2922, 2860, 1633, 1578, 1455, 1166, 1062, 987, 986, 856, 810, 776, 727, 701, 672, 642$ cm^{-1} ; $^1\text{H-NMR}$ (CDCl_3 , 400 MHz): $\delta = 2.28$ (dd; $J = 2.2, 13.96$ Hz, 1H, H-12), 2.74 (dd; $J = 2.2, 13.92$ Hz, 1H, H-12), 4.36 (t; $J = 2.2$ Hz, 1H, H-10), 5.83 (s; 1H, H-9), 7.10–7.22 (m; 6H, ArH) ppm; $^{13}\text{C-NMR}$ (CDCl_3 , 100 MHz): $\delta = 43.8, 46.3, 48.4, 54.2, 122.1, 122.3, 127.5, 127.8, 129.2, 132.2, 132.9, 134.1, 134.4, 142.9, 143.7$ ppm.

3.2. Single-Crystal X-ray Diffraction of Isomer **1**

A colorless single crystal of isomer **1** with dimensions of 0.55 \times 0.38 \times 0.12 mm was selected for X-ray diffraction analysis. The X-ray diffraction data were collected on a Bruker APEX-II D8 VENTURE diffractometer [100(2) K] (Bruker AXS Inc., Billerica, MA, USA) equipped with a graphite monochromated Mo $\text{K}\alpha$ radiation ($\lambda = 0.71073$ \AA) source using ϕ and ω scans. A total of 16,403 reflections were collected with $\theta_{\text{max}} = 27.5^\circ$ and $\theta_{\text{min}} = 2.3^\circ$; 3250 of them were independent with $R_{\text{int}} = 0.089$. The structure was solved using the direct method with SHELXT [31], and refined using the full-matrix least squares method on F2 with anisotropic thermal parameters for all non-hydrogen atoms using SHELXL-97 [32]. All hydrogen atoms were located theoretically and refined with riding model position parameters and fixed isotropic thermal parameters. Details of the data collection conditions and the parameters of the refinement process are given in Table 1.

3.3. Theoretical Calculations

The structures of **1** and **2** were optimized using the DFT/B3LYP method for minimum energy geometries with no imaginary frequency. The 6-31G(d,p) basis set was used as implemented in the Gaussian 03 software (Gaussian, Inc., Wallingford, CT, USA) [33]. For the optimized structures, the HOMO and LUMO were drawn using the GaussView software [34]. Also, the electron density maps based on the MEPs of the two regioisomers were drawn using the same software.

4. Conclusions

4,5,12- and 1,8,12-trichloro-9,10-dihydro-9,10-ethanoanthracene-12-carbonitriles, **1** and **2**, were synthesized easily and successfully characterized using ^1H - and ^{13}C -NMR, and IR spectroscopic techniques. The three-dimensional structure of isomer **1** was further confirmed using a single crystal

X-ray technique. Using DFT calculations at the B3LYP level of theory and the 6-31G(d,p) basis set, the relative stabilities, molecular structures and electronic properties of **1** and **2** were deduced. Isomer **1** is more thermodynamically stable than isomer **2** in the gas phase and in solution. Based on the Gibbs free energy analysis, isomer **1** could be considered thermodynamically more stable than **2**.

Acknowledgments: The authors extend their sincere appreciation to the Deanship of Scientific Research at the King Saud University for its funding this Prolific Research group (PRG-1437-29).

Author Contributions: M.A.S., U.K., Y.N.M., and A.I.A. conceived and designed the experiments; M.A.S. performed the experiments; M.A.S., and U.K. analyzed the data; H.A.G. carried out the single-crystal structure determination; S.M.S. carried out the DFT calculations; and M.A.S., S.M.S., and H.A.G. wrote the paper.

Conflicts of Interest: The authors declare no conflict of interest.

References

1. Wadler, S.; Fuks, J.Z.; Wiernik, P.H. Phase I and II agents in cancer therapy: I. Anthracyclines and related compounds. *J. Clin. Pharmacol.* **1986**, *26*, 491–509. [[PubMed](#)]
2. Sunmonu, T.O.; Owolabi, O.D.; Oloyede, O.B. Anthracene-induced enzymatic changes as stress indicators in African catfish, *Heterobranchus bidorsalis* Geoffroy Saint Hilaire, 1809. *Res. J. Environ. Sci.* **2009**, *3*, 677–686.
3. Lee, A.H.; Jang, Y.; Kim, G.H.; Kim, J.J.; Lee, S.S.; Ahn, B.J. Decolorizing an anthraquinone dye by *phlebia brevispora*: Intra-species characterization. *Eng. Life Sci.* **2017**, *2*, 125–131. [[CrossRef](#)]
4. Varol, S.F.; Sayin, S.; Eymur, S.; Merdan, Z.; Ünal, D. Optical performance of efficient blue/near UV nitropyridine-conjugated anthracene (NAMA) based light emitting diode. *Org. Electron.* **2016**, *31*, 25–30. [[CrossRef](#)]
5. Huang, H.-S.; Lee, K.-Y.; Shi, C.; Hsu, H. Synthesis and Pharmaceuticals of Novel 9-Substituted-1, 5-Dichloroanthracene Analogs. U.S. Patent 6,369,246 B2, 9 April 2001.
6. Banerjee, A.K.; Giri, V.S.; Mukherjee, R.; Kapoor, K.K.; Desiraju, G.; Jaggi, M.; Singh, A.T.; Dutta, S.K.; Sairam, K.V. Hydroanthracene Based Compounds as Anticancer Agents. U.S. Patent 20,040,220,197 A1, 4 November 2004.
7. Bair, K.W. Anthracene Derivatives. U.S. Patent 4,803,221 A, 7 February 1989.
8. Rastinejad, F.; Foster, B.; Coffey, H.; Connell, R. Methods and Composition for Restoring Conformational Stability of a Protein of the p53 Family. U.S. Patent 20,020,048,271 A1, 23 May 2001.
9. Karama, U.S.; Sultan, M.A.S.; Tahir, K.E.H.E. Antidepressant Compounds. U.S. Patent 9,125,866 B1, 8 September 2015.
10. Cloonan, S.M.; Drozdzowska, A.; Fayne, D.; Williams, D.C. The antidepressants maprotiline and fluoxetine have potent selective antiproliferative effects against Burkitt lymphoma independently of the norepinephrine and serotonin transporters. *Leuk. Lymphoma* **2010**, *51*, 523–539. [[CrossRef](#)] [[PubMed](#)]
11. Szabó, D.; Szabó, G.; Ocsóvszki, I.; Aszalos, A.; Molnár, J. Anti-psychotic drugs reverse multidrug resistance of tumor cell lines and human AML cells ex-vivo. *Cancer Lett.* **1999**, *139*, 115–119. [[CrossRef](#)]
12. Bitonti, A.J.; Sjoerdsma, A.; McCann, P.P.; Kyle, D.E.; Oduola, A.; Rossan, R.N.; Milhous, W.K.; Davidson, D.E. Reversal of chloroquine resistance in malaria parasite *Plasmodium falciparum* by desipramine. *Science* **1988**, *242*, 1301–1303. [[CrossRef](#)] [[PubMed](#)]
13. Cloonan, S.M.; Williams, D.C. The antidepressants maprotiline and fluoxetine induce type II autophagic cell death in drug-resistant Burkitt's lymphoma. *Int. J. Cancer* **2011**, *128*, 1712–1723. [[CrossRef](#)] [[PubMed](#)]
14. Stockdale, T.P.; Williams, C.M. Pharmaceuticals that contain polycyclic hydrocarbon scaffolds. *Chem. Soc. Rev.* **2015**, *44*, 7737–7763. [[CrossRef](#)] [[PubMed](#)]
15. Brocksom, T.J.; Nakamura, J.; Ferreira, M.L.; Brocksom, U. The Diels-Alder reaction: An update. *J. Braz. Chem. Soc.* **2001**, *12*, 597–622. [[CrossRef](#)]
16. Nicolaou, K.C.; Snyder, S.A.; Montagnon, T.; Vassilikogiannakis, G. The Diels–Alder reaction in total synthesis. *Angew. Chem. Int. Ed.* **2002**, *41*, 1668–1698. [[CrossRef](#)]
17. Diels, O.; Alder, K. Synthesen in der hydroaromatischen reihe. *Justus Liebigs Ann. Chem.* **1928**, *460*, 98–122. [[CrossRef](#)]

18. Sultan, M.A.; Karama, U. Substituent effects on regioselectivity of the Diels-Alder reactions: Reactions of 10-allyl-1,8-dichloroanthracene with 2-chloroacrylonitrile, 1-cyanovinyl acetate and phenyl vinyl sulfone. *J. Chem.* **2016**, *5*. [[CrossRef](#)]
19. Phutdhawong, W.; Buddhasukh, D. Facile microwave-assisted synthesis of 9, 10-dihydro-9, 10-ethanoanthracene-11-carboxylic acid methyl ester. *Molecules* **2005**, *10*, 1409–1412. [[CrossRef](#)] [[PubMed](#)]
20. Atherton, J.; Jones, S. Diels-Alder reactions of anthracene, 9-substituted anthracenes and 9, 10-disubstituted anthracenes. *Tetrahedron* **2003**, *59*, 9039–9057. [[CrossRef](#)]
21. Singh, M.D.; Ningombam, A. Diels-Alder reaction of 9-anthracenemethanol and dimethylacetylenedicarboxylate; potential route for the synthesis of regiospecific products of 9-substituted anthracene with unsymmetrical. *Indian J. Chem.* **2010**, *49*, 77–83.
22. Singh, M.D.; Ningombam, A. High stereoselectivity in the Diels-Alder reaction of substituted anthracenes: Reactions of 1-succinimidoanthracene and 1-phthalimidoanthracene with maleic anhydride. *Indian J. Chem.* **2010**, *49*, 789–794. [[CrossRef](#)]
23. Khan, R.; Singh, T.P.; Singh, M.D. Highly regioselective Diels-Alder reaction of 9-substituted anthracenes with citraconic anhydride. *Synlett* **2014**, *25*, 696–700. [[CrossRef](#)]
24. Wise, K.E.; Wheeler, R.A. Donor-acceptor-assisted diels-alder reaction of anthracene and tetracyanoethylene. *J. Phys. Chem. A* **1999**, *103*, 8279–8287. [[CrossRef](#)]
25. Karama, U.S.; Sultan, M.A.S.; Tahir, K.E.H.E.; Almansour, A.I. Halogenated Tetracyclic Compounds. U.S. Patent 9,498,460 B1, 22 November 2016.
26. Karama, U.; Sultan, M.A.; Almansour, A.I.; El-Taher, K.E. Synthesis of chlorinated tetracyclic compounds and testing for their potential antidepressant effect in mice. *Molecules* **2016**, *21*, 61. [[CrossRef](#)] [[PubMed](#)]
27. Sultan, M.A.; Karama, U.; Almansour, A.I.; Al-saedi, A.; Ghabbour, H.A. Crystal structure of 9-allyl-4, 5-dichloro-12-cyano-9, 10-dihydro-9, 10-ethanoanthracen-12-yl acetate, C₂₂H₁₇Cl₂NO₂. *Z. Krist.-New Cryst. Struct.* **2016**, *231*, 801–803.
28. Verma, S.M.; Singh, M.D. Structural elucidation with nuclear magnetic resonance spectroscopy. Diels-alder adducts of 1-aminoanthracene and maleic anhydride: Restricted rotation about the aryl C (1)-N bond and intrinsic asymmetry about the imide (Nsp²-Csp³) system. *J. Org. Chem.* **1977**, *42*, 3736–3740.
29. Kaplan, F.; Conroy, H. Electronic effects on the stereochemistry of the Diels-Alder reaction. *J. Org. Chem.* **1963**, *28*, 1593–1596. [[CrossRef](#)]
30. House, H.O.; Koepsell, D.; Jaeger, W. Derivatives of 1, 8-diphenylanthracene. *J. Org. Chem.* **1973**, *38*, 1167–1173. [[CrossRef](#)]
31. Sheldrick, G.M. *SHELXTL. Version 6.12 for Windows NT*; Bruker AXS Inc.: Madison, WI, USA, 2008.
32. Bruker. *SMART, Version 5.625 for Windows NT*; Bruker AXS Inc.: Madison, WI, USA, 2000.
33. Frisch, M.; Trucks, G.; Schlegel, H.; Scuseria, G.; Robb, M.; Cheeseman, J.; Montgomery, J., Jr.; Vreven, T.; Kudin, K.; Burant, J. *Gaussian 03, Revision c. 02*; Gaussian, Inc.: Wallingford, CT, USA, 2004.
34. Dennington, R.; Keith, T.; Millam, J. *Gauss View, Version 5*; Semicem Inc.: Shawnee Mission, KS, USA, 2009.

